PERGAMON

Journal of Structural Geology 22 (2000) 795–809

JOURNAL OF STRUCTURAL GEOLOGY

www.elsevier.nl/locate/jstrugeo

Garnet plasticity in the lower continental crust: implications for deformation mechanisms based on microstructures and SEM-electron channeling pattern analysis

R. Kleinschrodt [a,*], A. McGrew [b]

[a] *Institute for Mineralogy and Geochemistry, Universität zu Köln, Zuelpicher Str. 49b, D-50674, Köln, Germany*
[b] *Department of Geology, University of Dayton, 300 College Park, Dayton, OH 45469-2364, USA*

Received 5 May 1998; accepted 21 December 1999

Abstract

Elongated garnets which preserved deformational microstructures (boudinage, pinch and swell structures) occur in granulite facies quartzites in the Highland Complex of Sri Lanka. In spite of these microstructures and in contrast with previous reports on garnet plasticity, there are no or only few signs of intracrystalline deformation like subgrains or lattice distortion. This can be explained by annealing and slow static cooling from high temperatures. SEM-electron channeling pattern analysis reveals that the garnets have a significant crystallographic preferred orientation. Aspect ratio/grain-size analysis shows that the deformation mechanism is grain-size sensitive. These features indicate a diffusion assisted dislocation glide mechanism with dominant 1/2 $<111>$ {110} slip system. A comparison of the deformation behavior between garnet, quartz and feldspar shows, that differences in flow strength are low under the high-grade conditions (850 ± 50°C). Garnet is still the phase with the highest flow strength, but (dry) quartz is slightly stronger than feldspar.

1. Introduction

As garnets commonly form rigid objects during deformation of crustal and mantle rocks, they are generally thought to have a high creep strength compared to matrix forming minerals such as quartz and feldspar in the crust and olivine in the mantle. Experimental deformation of garnets corroborates this observation and the high strength of the garnets is explained by high resistance to dislocation glide due to the very large Burgers vectors (Karato et al., 1995). Nevertheless, there have been a few reports that argue for garnet ductility in naturally deformed crustal rocks (Dalziel and Bailey, 1968; Ross, 1973; Ji and Martignole, 1994). Orientation contrast (OC) images reveal that garnets frequently show numerous substructures (subgrains) (Prior et al., 1998). This suggests that dislocation creep is the dominant deformation mechanism (Prior et al., 1996). Voegele et al. (1998) showed that garnets in high-T eclogites show microstructures characteristic of dislocation creep with recovery.

A recent discussion on the deformation mechanisms controlling plastic deformation of garnet under natural conditions (den Brok and Kruhl, 1996; Ji and Martignole, 1996) shows that there is still considerable debate in the interpretation of garnet microstructures and that well-constrained examples of plastically deformed garnets are rare.

In this paper we present deformed garnets from granulite facies metasediments of the Highland Complex of Sri Lanka. Compared to the reports cited above, these garnets are unique because their shapes have preserved deformational microstructures acquired during high-T deformation (750–850°C) without later deformational overprint. We use microstructural data, digital image analysis and garnet textures measured by means of SEM electron channeling pattern analysis to

* Corresponding author.
E-mail address: kleinsch@min.uni-koeln.de (R. Kleinschrodt).

0191-8141/00/$ - see front matter
PII: S0191-8141(00)00010-9

constrain deformation mechanisms active during natural plastic deformation of garnets.

2. Geological setting

The granulite facies Highland Complex forms the N–S-trending central backbone of Sri Lanka and is flanked by amphibolite facies units to the east and west (Fig. 1). It consists of numerous charnockite layers intercalated in a supracrustal sequence of granulites. This sequence is formed by a variety of metasedimentary rocks including marbles, calcsilicate granulites, metapelitic granulites and quartzites. Some of these layers can be traced for tens of kilometers.

Peak metamorphic temperatures of 850–900°C at pressures of about 8–9 kbar (Schumacher et al., 1990; Schumacher and Faulhaber, 1994) (Fig. 2) were reached at about 610–600 Ma (Hölzl et al., 1994). During peak conditions a granulite facies foliation (S_1) formed associated with a pronounced stretching lineation, representing the main fabric elements in the Highland Complex. This stretching lineation is marked by long axes of quartz and feldspar grains, *c*-axes of hornblende, pyroxene and sillimanite, and long axes of all recrystallized aggregates. Isoclinal refolding of S_1 with axes parallel (D_2) and normal to the stretching lineation (D_3) occurs locally with stable peak metamorphic assemblages (other authors label all isoclinal folding D_2, independent of the orientation of the fold axes). Locally, high-strain zones are mappable parallel to the dominant foliation S_1 with a thickness up to 200–400 m. Large scale synforms and antiforms (D_4) with upright or slightly W-dipping axial planes formed during or after isobaric cooling to about 750°C (Fig. 2), but before significant decompression, and mark the last penetrative deformation in the central Highland Complex. Prior to D_4, foliation in the Highland Complex was subhorizontal, and is still subhorizontal where D_4 is missing, for example, in the southern Highlands of Sri Lanka.

Spectacular elongate garnets have been found in one of these large scale D_4-synforms, the Dumbara Synform east of Kandy, but they may be more widespread. The garnets occur within quartzites situated in the marginal part of an S_1-parallel high-strain zone known as the Digana movement zone (Kleinschrodt et al., 1991). Several quartzite horizons up to 50 m thick occur in a sequence of metasedimentary granulites. The sample localities of the garnets treated in this paper are indicated in Fig. 1. They lie in the deeper, outer part of the sequence exposed in the Dumbara Synform. As pointed out in a paper on the tectonometamorphic evolution of the Dumbara Synform

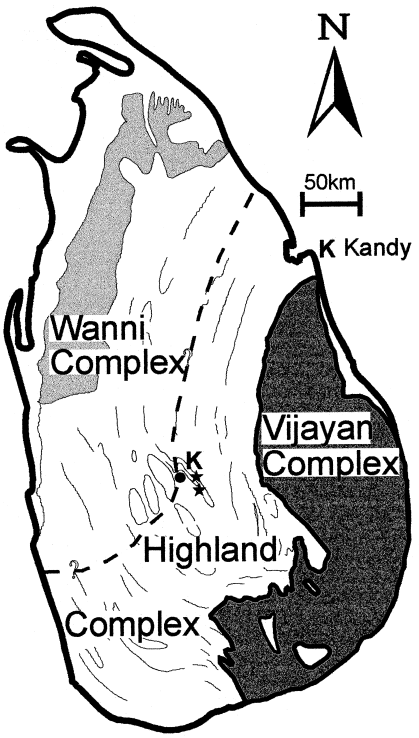

Fig. 1. Main geological units of Sri Lanka according to the Geological Map of Sri Lanka (1984). The dashed line with question marks indicates the extended boundary of the Wanni Complex by Kröner et al. (1991). Asterisks indicate collection localities for deformed garnet bearing quartzites.

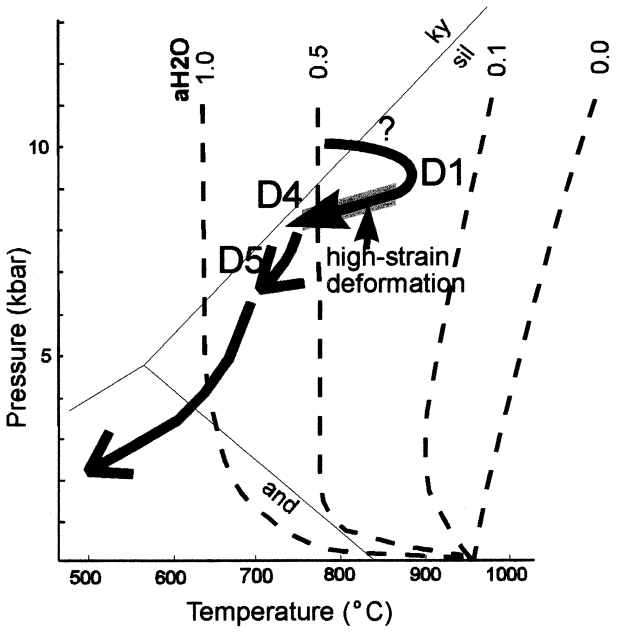

Fig. 2. *P–T*-path of granulites from the Highland Complex, compiled from Schuhmacher et al. (1990) and Kleinschrodt and Voll (1994) with correlated deformation events: D_1: formation of the main foliation, D_4: formation of the large scale synforms and antiforms (post high-strain deformation), D_5: thrusting of the Highland Complex on top of the Vijayan Complex.

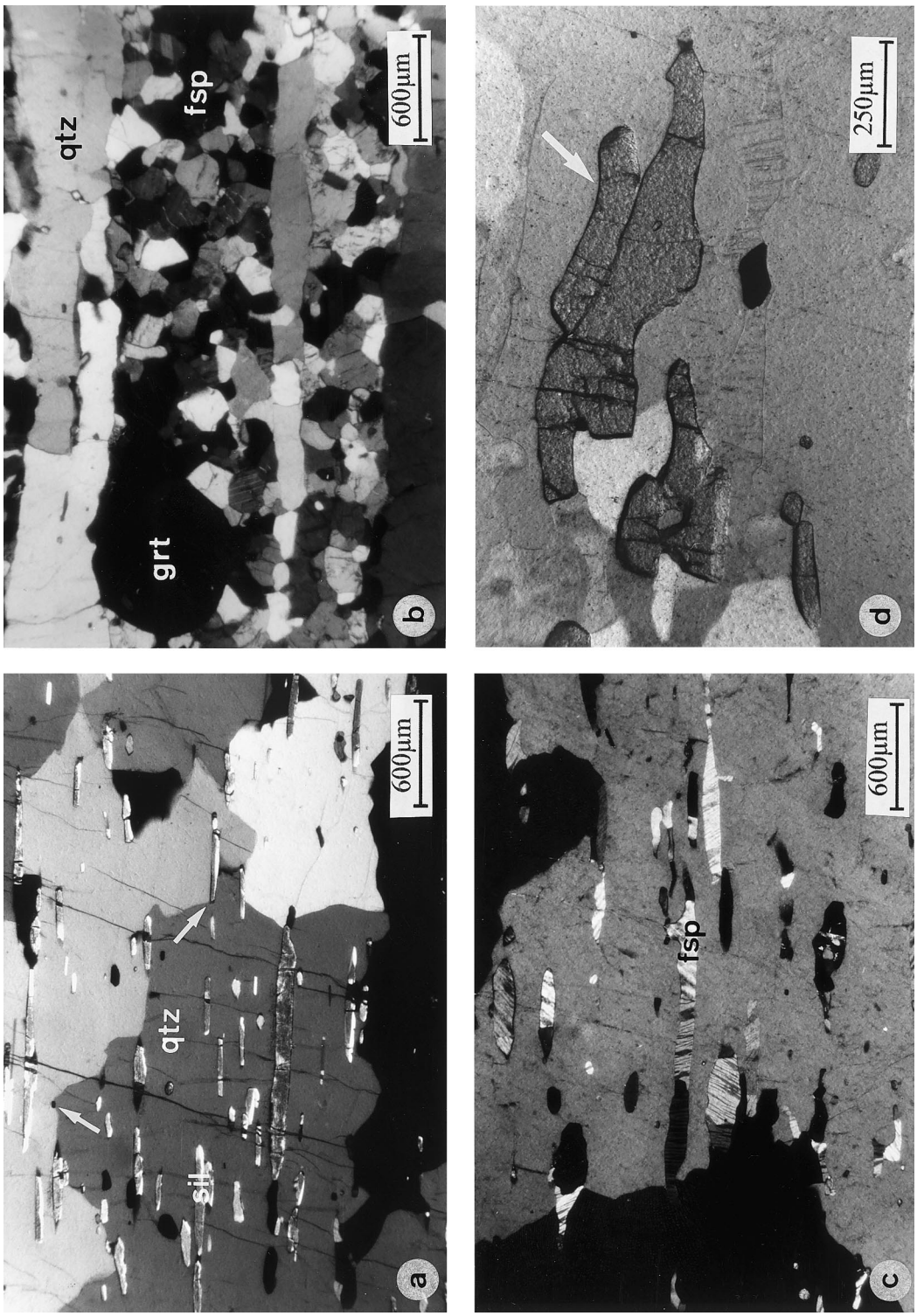

Fig. 3. Quartz and feldspar fabrics in XZ sections: (a) Large strain-free quartz grains with irregular grain boundaries often pinned at phase boundaries (arrows). Additional phases are sillimanite, magnetite and zircon. (b) Quartz lamellae between recrystallized feldspar layers. Note the equant shape of garnet (dark phase to the left) in the feldspar layer. (c) Lensoid alkali-feldspars in large quartz grain. The feldspars show albite-rich exsolution lamellae (dark lamellae in fsp), i.e. they were deformed as solid-solutions and exsolved after deformation. (d) A garnet fractured at the end of the high-strain event. Fragments to the left and in the center have already drifted apart. A tabular fragment is starting to peel off and separate in the top of the central garnet (arrow).

(Kleinschrodt and Voll, 1994), at this deeper level, folding is not accompanied by a penetrative cleavage on the limbs of the fold.

Garnet–orthopyroxene assemblages in basic layers a few tens of meters above the quartzite sequence from the western limb of the Dumbara synform yield peak condition P–T values like those mentioned above, even though they are slightly affected by an S_4 cleavage

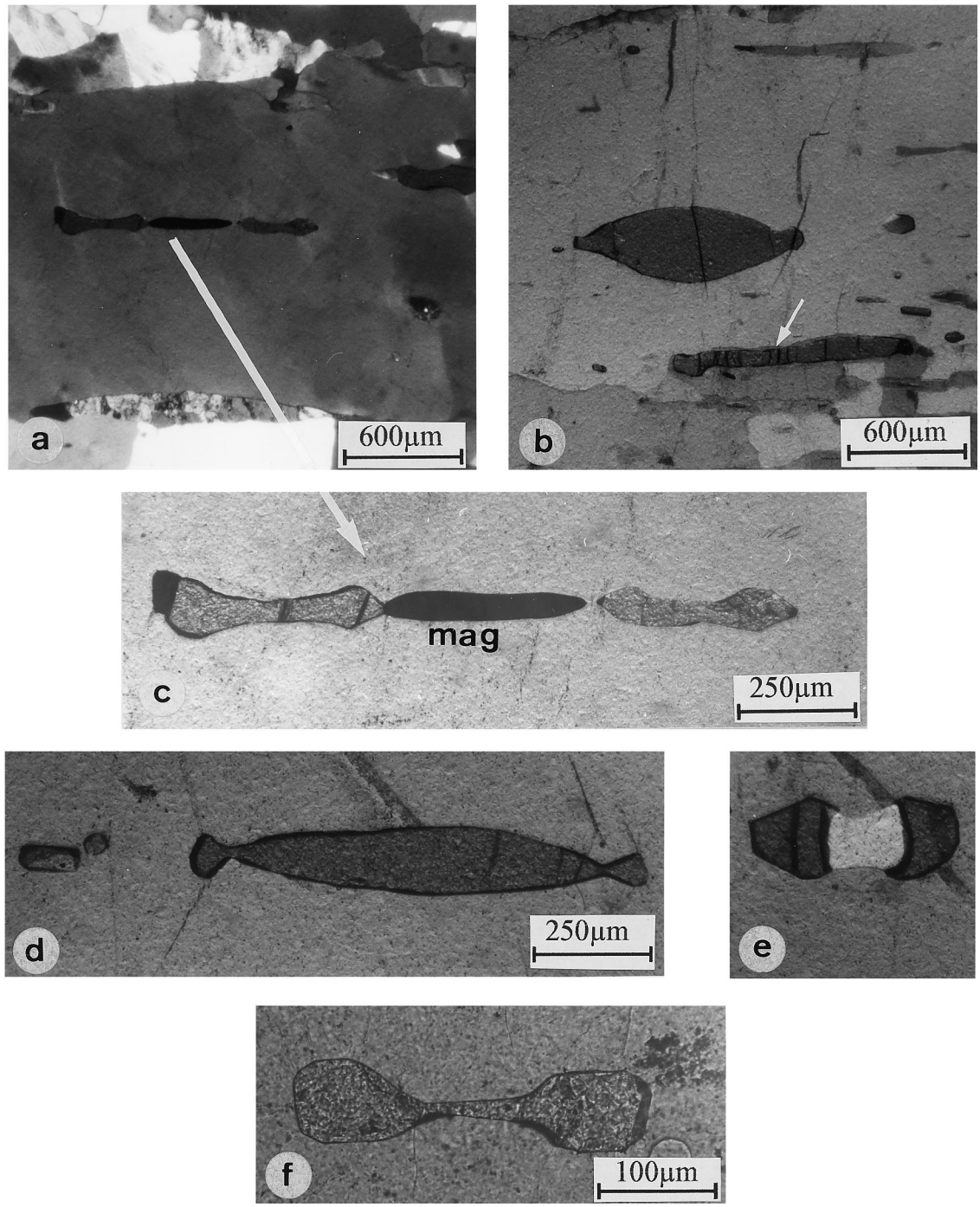

Fig. 4. Garnet shapes in quartzites. (a) Large quartz grain including elongated garnets and magnetite. Few subgrains and minor undulatory extinction in quartz. Crossed polarized light. Close up in (c). (b) A lensoid garnet in the central part with a small fragment to the right, probably derived from the larger grain. The strongly elongate garnet in the lower part is rimmed by feldspar (arrow), which may indicate an origin from metamorphic reaction from a former elongate grain. Such garnets were not included in the measurements. Plane polarized light (PPL). (c) Close-up of (a), showing comparable aspect ratios in a magnetite in the center and in the garnets to the left and right, PPL. (d) Peculiar garnet with lensoid center and pinched parts to each side. The fragment to the left may originate by complete pinching of and drifting away from the larger garnet, PPL. (e) Boudinaged, fish-mouth-shaped garnet, PPL. (f) Dumb-bell-shaped garnet, PPL.

during the formation of the large scale fold (Kleinschrodt and Voll, 1994). A lower limit for the high strain deformation is set by feldspar thermometry on a pegmatoid dyke which crosscuts the high-strain zone and yields a lower limit of 759°C or 705°C (depending on which calculation mode is used, Voll et al., 1994). Furthermore, recalculating the feldspar composition of the exsolved K- and Na-feldspars, which were deformed as homogeneous solid solutions, also gives a minimum temperature for the formation of the high-strain zone that is well above 700°C. In summary, the temperature during deformation is between 750 and 850°C.

3. Microfabrics

3.1. The matrix

Compositional banding in the quartzites is defined by changing feldspar content and concentrations of heavy minerals. Grain size in the quartzites is coarse with individual grains up to 10 cm in diameter. Grain boundaries are irregular and coarsely serrated and often pinned to other phases (sillimanite, magnetite, garnet, feldspar) (Fig. 3a, c). The coarse grain-size is due to post-tectonic grain growth during slow cooling (2–3°C/Ma, Kleinschrodt and Voll, 1994) from high temperature (approximately 700–750°C). Whereas quartz has lost its shape preferred orientation in quartzitic layers, it is preserved where quartz is enclosed in layers of feldspar. In such layers quartz forms lenses elongate in L_1, composed of one or a few grains (Fig. 3b), while feldspar forms similar lenses when it is enclosed in quartz (Fig. 3c). They either form elongate monocrystalline lenses or equant polygonal grains in polycrystalline lensoid aggregates. Higher feldspar contents are usually correlated with the formation of feldspar layers, which in turn include long quartz lenses or lamellae (Fig. 3b). Large quartz grains typically show almost no undulatory extinction and few optically visible subgrains (Figs. 3a and c, 4a). Subgrains are rectangular or approximately quadratic in shape with subgrain boundaries oriented (sub-)parallel and (sub-)normal to $<c>$. As quartz is a very sensitive monitor of stress, these large grains with little or no intracrystalline strain demonstrate that exhumation was accompanied by very little deformation.

3.2. The garnets

Garnets are a common phase forming about 2–5 volume percent and with a grain size up to the centimeter scale. The macroscopically dominant garnets generally are subequant with only slight shape preferred orientation, with long axes parallel to the stretching lineation. Aspect ratios of these garnets in XZ sections generally are less than X:Z = 2. Garnets may include round quartz or long-prismatic sillimanite. Smaller garnets (Fig. 4) visible in thin sections show significant shape preferred orientations. Several features indicate plastic deformation of the garnets. Characteristics of the deformed garnets are compiled in Fig. 3 and include: dumb-bell-shaped garnets with thinning in the central part (Fig. 4a, c, f,); strongly elongate grains with high aspect ratios (Fig. 4b, d); lensoid shapes, with tails thinning in S_1 (Fig. 4b); 'fish-mouth-shaped' boudinage structures (Fig. 4e); and pinch and swell structures (Fig. 4d).

The example in Fig. 4(d) shows that at both tips of the garnet, small segments are close to being separated from the main garnet. Small garnets with low aspect ratios like the one at the left side of Fig. 4(d) may result from such a process of plastic segmentation (the term segmentation is preferred here, as it is not a brittle fracturing, therefore not a fragmentation) followed by drifting away from the main parent garnet. Often several such segments are lined up in the stretching direction. The shape features of the deformed garnets resemble magnetites deformed together with the garnets (Fig. 4a, c).

4. Grain-size and aspect ratios

4.1. Garnets

The shapes of the garnets have been analysed in XZ and YZ sections in identical layers of sample 3164 and are compiled in Fig. 5. The slope of the regression line calculated for the measured data is regarded as an average Z/X or Z/Y value. The garnet population smaller than 0.2 mm^2, which is incorporated in Fig. 5(a and b), is displayed separately in Fig. 5(c and d). The aspect ratios for small garnets are significantly higher than those for the total population.

Every grain-size and grain shape analysis from two-dimensional sections through a three-dimensional rock fabric has to regard the possible influence of a cut effect. The general shape of the garnets is a disk extended in the stretching lineation. As not all of them are cut through their centers one would expect that grains which are cut marginally (i.e. which have a smaller apparent grain size) have lower or similar X/Z or Y/Z aspect ratios than a central section, in no case a larger one. As we found increasing aspect ratios with decreasing grain size, this cannot be caused by a stereological effect. The true aspect ratios could even be higher.

In Fig. 6(a and b) the aspect ratios are plotted against the area of individual garnets cut by the thin sections (not as usually done recalculated to an

average spherical grain radius). In XZ-sections aspect ratios up to 10 have been measured. Significantly elongated garnets (aspect ratios higher than 4) occur only at grain-sizes less than 0.4 mm^2 in thin sections (corresponding to a calculated spherical grain radius of about 350 μm) and only within a quartz matrix. Larger garnets show only slight shape preferred orientation with low aspect ratios, generally less than X/Z = 2. Although there is no simple linear correlation between grain size and aspect ratios, it seems clear that high aspect ratios are strongly dependent on small grain sizes. The correlation between grain size and aspect ratio may be disturbed by a process of segmentation during which smaller, more equant 'daughter grains' shear off and drift away from initially longer 'parent grains' (Fig. 4d). This causes the occurrence of numerous small grains with low aspect ratios. These grains are not formed by grain-boundary reduction during annealing but during deformation of the garnets.

The process of garnet fragmentation/segmentation probably occurred during several stages of deformation. Firstly, brittle fragmentation of larger garnet grains may play an important role in effectively

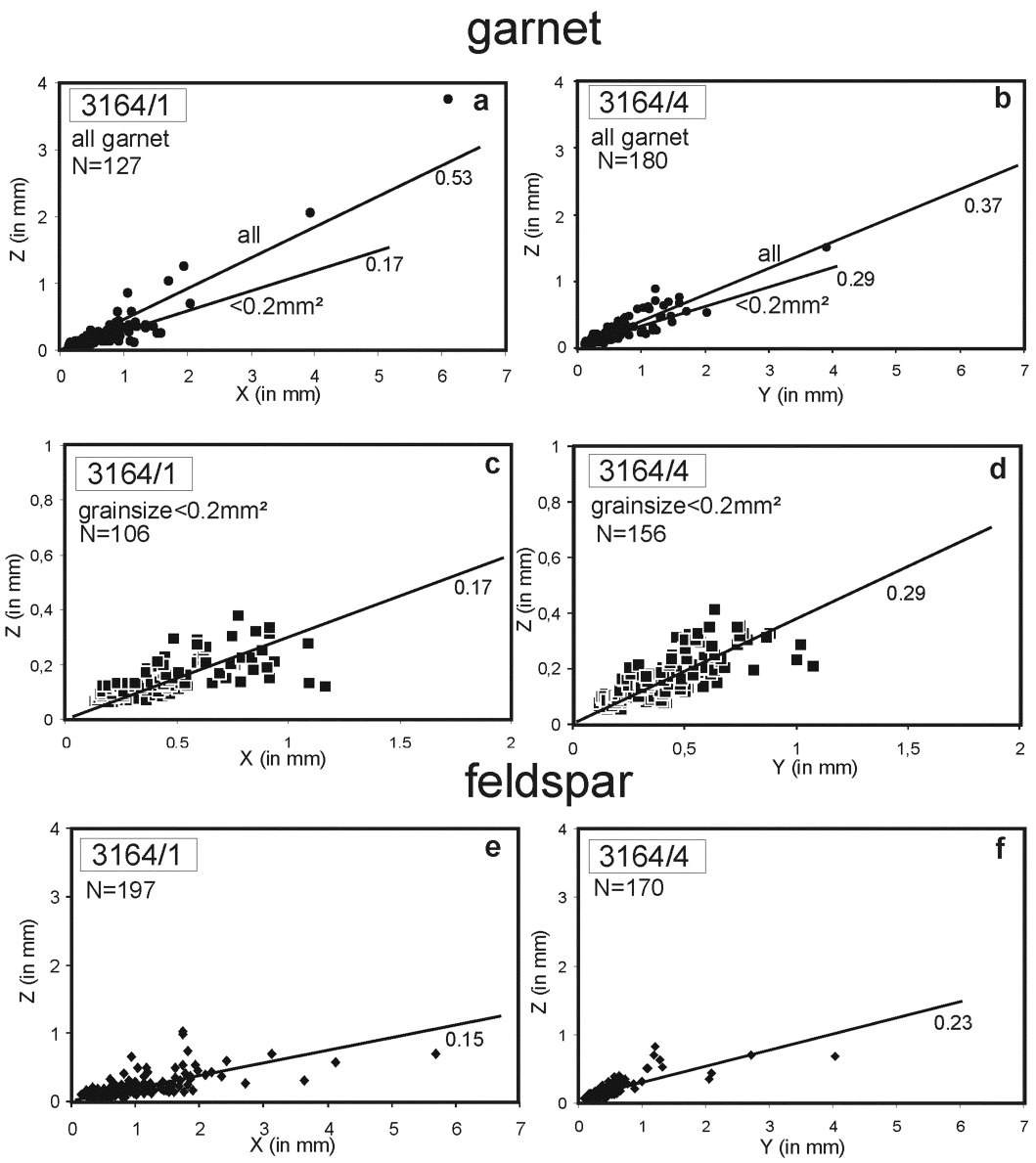

Fig. 5. Aspect ratios of garnets (a–d) and feldspars (e and f) in quartz matrix in XZ and YZ sections from sample 3164. Regression lines are plotted, their slopes are indicated below their right end. The total garnet populations are plotted in (a) and (b) [the lower regression line was calculated for grain-size < 0.2 mm^2, identical to regression lines in (c) and (d)], garnets with grain size < 0.2 mm^2 are additionally plotted in separate diagrams (c) and (d). *N*: Number of measured grains.

reducing garnet grain size and producing tabular initial grain shapes. We follow Gregg (1978) in suggesting that this initial phase of fragmentation could be accomplished through shear sliding on a set of fractures during rotational deformation, thus producing a series of tabular grains that would slide against each other as they rotate and eventually drift apart as deformation progressed. Ji and Martignole (1994) also considered but eventually rejected this as an effective mechanism in their rocks because the fragments do not show the features that Gregg (1978) considered to be critical: i.e. the grains are not angular; they cannot be fitted back together to form an original parent grain; the grains are not free of subgrains. However, if fragmentation preceded plastic high-strain deformation, then none of these arguments apply. In our rocks, tabular fragments are locally found frozen in a state of initial separation (Fig. 3d), suggesting that such a fracture mechanism may in part be responsible for a tabular grain shape. A second phase of segmentation of garnet grains occurred during plastic deformation through a process of pinching off and drifting away of smaller grains described above (see Section 4.3).

The average X/Z and Y/Z values (derived by regression analysis like in Fig. 5) measured for layers differing in quartz grain size (due to different feldspar contents) of sample 3164 were converted to X/Y and Y/Z ratios and plotted in a Flinn diagram (Fig. 6c); because of unknown initial shape and possible volume change, the latter is not thought to reflect finite strain values. The garnets plot close to the plane strain axis. A comparison of garnets deformed in a quartz matrix and in a feldspar matrix of closely adjacent layers yields significantly lower aspect ratios for the garnets deformed in the feldspar matrix. In XZ sections an average value of $X/Z = 1.8$ was obtained. The garnets in a feldspar matrix plot close to the origin, slightly within the oblate field.

4.2. Feldspar

Alkali-feldspar and plagioclase occur as monocrystalline lenses or polycrystalline aggregates, ribbons or layers within the quartzites together with the garnets described above (Fig. 3). Their long axes are strictly parallel to the stretching lineation. Monocrystalline lenses of alkali-feldspar, later exsolved to coarse flame perthite, are found enclosed in much larger quartz grains, which enveloped the feldspars during post-deformational static grain growth. These lenses have preserved the shape preferred orientation whereas in feldspar layers it has been modified by static grain

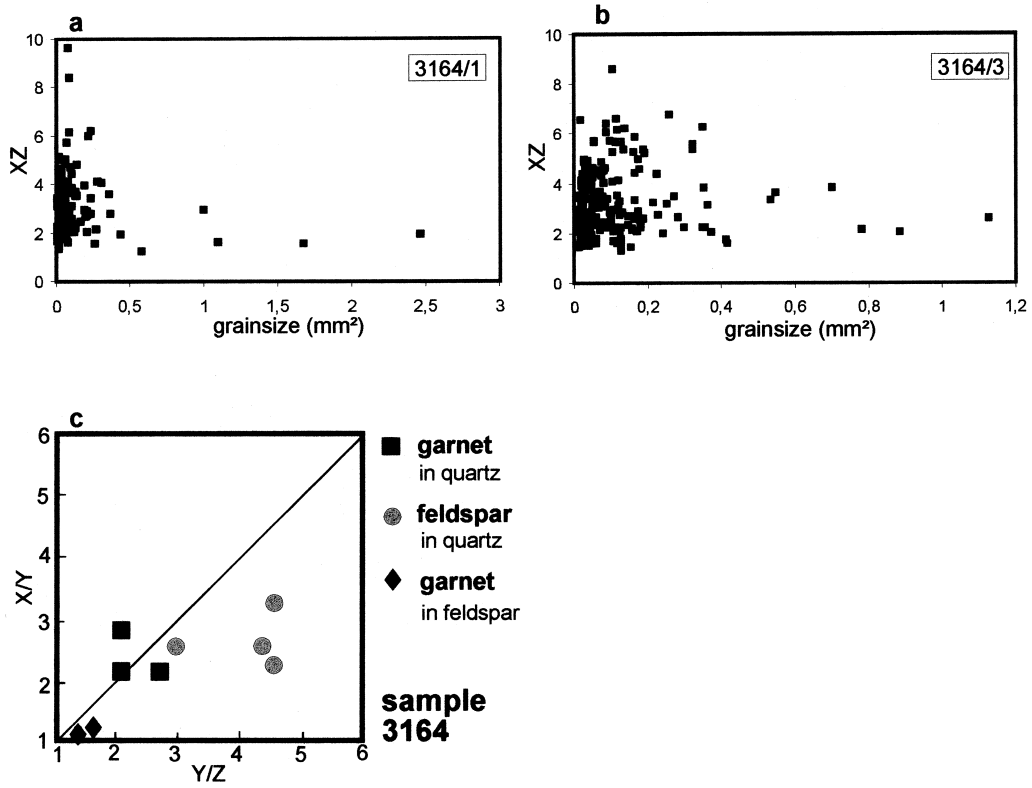

Fig. 6. (a) and (b) Grain size vs. aspect ratios in XZ sections from two domains of different quartz grain size (due to different feldspar and sillimanite content) of sample 3164. (c) X/Y vs. Y/Z plot (Flinn diagram) of garnet and feldspar aspect ratios from different domains of sample 3164. Each point was derived by regression analysis of aspect ratio measurements in XZ- and YZ-sections.

growth of the feldspars themselves. Where the shape preferred orientation of feldspar is preserved, aspect ratios up to 13 in XZ sections were measured. Compared to garnets, the feldspars show higher aspect ratios (Fig. 5e and f) and the average values derived from XZ and YZ sections plot in the oblate field of a Flinn diagram (Fig. 6c), although again we note that the interpretation of this observation is complicated by the possibility of an initial shape preferred orientation (see below).

4.3. Comparison of garnet, quartz and feldspar shape anisotropy

Ji and Martignole (1994) use the apparent strain difference from the Flinn diagram to infer that garnet is weaker than quartz and feldspar. According to Freeman and Lisle (1987), the more oblate form of the garnets observed in their rocks argues for garnets being weaker than feldspars in a quartz matrix. The measurements in our rocks show a different result. The feldspar grains are more oblate than garnets in a quartz matrix. Comparing the fabrics from the Sri Lankan rocks with those from the Morin shear zone, it is evident that the rocks from Sri Lanka preserved the state of static grain coarsening at temperatures of about 750 ± 50°C. Quartz grains show few or no subgrains, despite their large grain size. Where subgrains are present, they are coarse with subgrain boundaries about normal to the $<c>$- and $<a>$-directions. Subgrains, recrystallized grains and strain-induced boundary migration formed at (750–550°C), which overprint a coarse grained high-T quartz fabric (>900°C) are clearly shown in Ji and Martignole (1994, figs. 2 and 3). Consequently, there seems to be no justification for correlating the strain in the feldspar (which can be readily deformed in the temperature range of 550–750°C) with the garnet strain in these rocks. Therefore, the conclusion that garnet is softer than feldspar and quartz during the high-temperature event is misleading.

The question arises as to whether it is justifiable to compare strain between garnet and feldspar in our samples, which only suffered the high-temperature deformation followed by slow static annealing and cooling from about 750°C. The crucial point is the initial shape of feldspar and garnet at the moment when plastic deformation of the garnets started. Arguments for the latter must include the following observations:

1. Quartzites outside the high-strain zone include feldspars with, on average, low aspect ratios in the range of about X:Y:Z = 2–2.5:1.5:1. Feldspars are rarely equant shaped.
2. Garnet shapes are approximately isometric in many rock types in Sri Lanka and also in low-strain quartzites. As this is the common appearance of garnets in many metamorphic rocks, this misleads Ji and Martignole (1994) and den Brok and Kruhl (1996) in their discussion on the paper to accept an isometric shape of the garnets at the beginning of plastic deformation. However, in the high-strain zone this initial shape may be modified prior to plastic deformation by fracturing and shear sliding, producing smaller, tabular shaped garnets.

So, in neither of the latter cases can we postulate that the aspect ratios really reflect the plastic strain acquired during the timespan in which garnet can be plastically deformed, and this seems to be especially true for the rocks of Ji and Martignole (1994).

Although these uncertainties cannot be ignored, some observations seem to be particularly critical for a comparison of the relative flow strength of quartz, feldspar and garnet:

1. While garnet is deformed in a quartz matrix, it is not deformed or deformed only slightly in a feldspar matrix. In other words, the relative flow strength of garnet is greater in a matrix of feldspar than it is in a matrix of quartz and, therefore, the competency contrast between garnet and feldspar is higher than between garnet and quartz.
2. Quartz is deformed in a feldspar matrix and vice versa with only slight competency contrast.
3. From both statements it can be inferred, that even though the competency contrast between quartz and feldspar is small, the difference is high enough that garnet is significantly deformed in quartz and not in feldspar, i.e. the flow strength of quartz must be higher, closer to garnet flow strength than that of feldspar.

Summing up, garnet is the strongest phase, but the competency ratio compared to quartz is close to 1 and allows plastic deformation of the garnet. Feldspar seems to be the weakest phase, and the competency ratio of garnet relative to feldspar is high enough that garnet remains nearly undeformed in a feldspar matrix. Compared to lower temperature deformation, the competency contrast between all three phases is low.

5. Textures and deformation mechanisms

5.1. Methods

In order to evaluate deformation mechanisms, one sample from the central Highland Complex (sample 3164-2) was selected for detailed investigation by scanning electron microscope (SEM) electron channeling analysis. Electron channeling is a well established technique for determining the complete crystallographic

orientation of most minerals. The electron channeling pattern (ECP), and the crystallographic orientation of the grain that produces it can be determined (or indexed) by comparing the observed ECP with an ECP map for the mineral in question using sophisticated image analysis software such as the computer program Channel (Schmidt and Olesen, 1989). A full description of the technique is provided by Lloyd (1987, 1994).

For typical grain sizes, the effective scanning angle for each grain is so small that the angle of incidence is essentially constant over the area of each grain but varies from one grain or subgrain to the next. This results in an OC image in which the intensity of the back-scattered electron signal varies as a function of the crystallographic orientation of the grain in question (Fig. 7). Although OC images do not allow quantitative indexing of crystallographic orientations, they are nevertheless very useful because they provide an image of the microstructure that is analogous to a crossed polarized image under the optical microscope, except that the orientation contrast varies as a function of all crystallographic directions, not just the indicatrix axes directions. Consequently, OC images can be obtained even for minerals that are isotropic under the polarizing microscope, such as garnet.

5.2. Quartz

Quartz from the granulites of the central Highland Complex generally shows well-developed crystallographic preferred orientations, most commonly characterized by 90° crossed girdles with maxima at angles of 40–80° to the Y-axis (Kleinschrodt, 1994; Kleinschrodt, 1996a). Both the skeletal outlines and the maxima distributions are typically symmetrical. The same types of textures (used here synonymously with

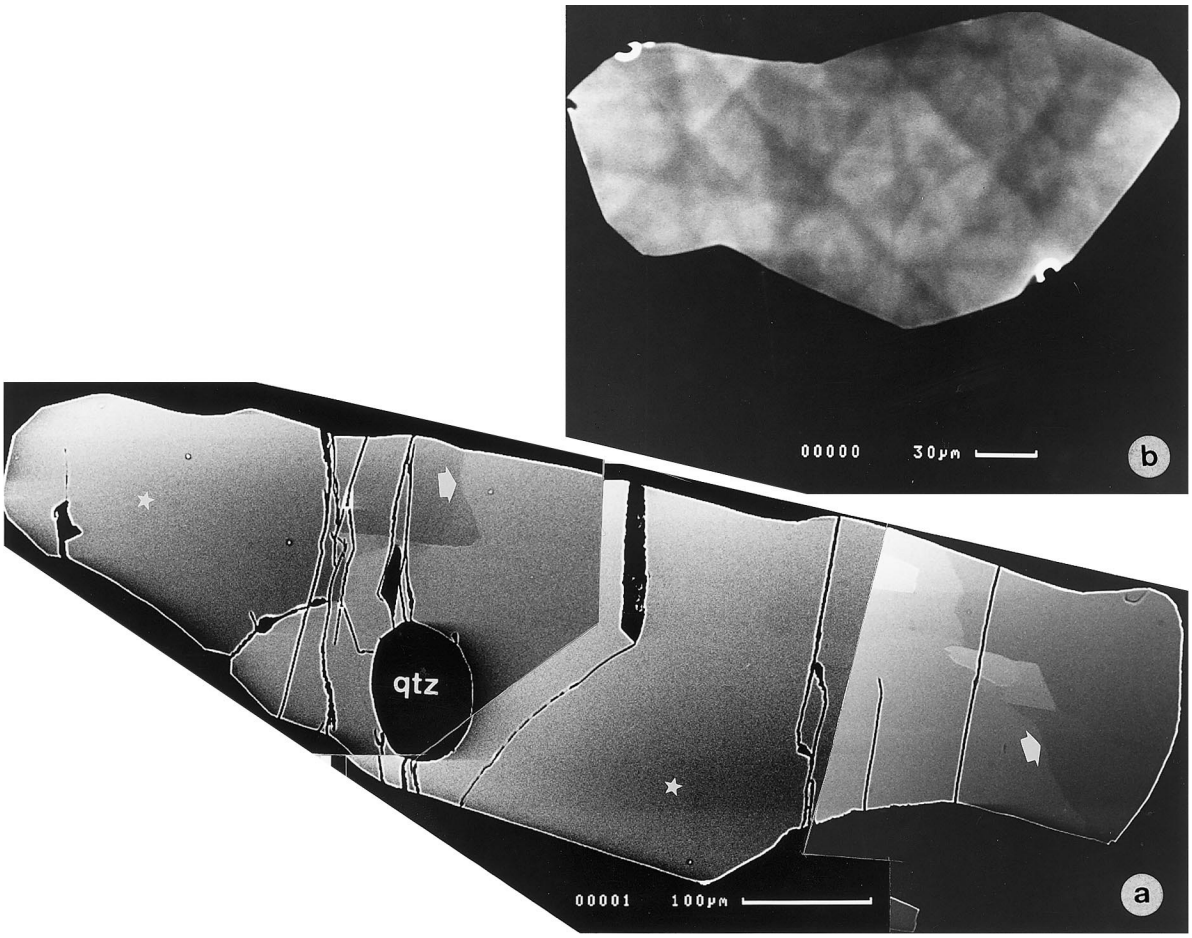

Fig. 7. (a) An orientation contrast photomontage of a single elongate garnet grain, which shows the most extensive subgrain development of any garnet grain observed in sample 3164-2 (the margins of the photographs are visible as straight contours). Subgrain boundaries marked by orientation contrast are indicated with arrows. Differences in brightness in the surroundings of the asterisks are imaging artefacts. Although this photomicrograph clearly provides evidence for a certain amount of dislocation activity, even in this case, subgrains are few and relatively coarse. Also present in this garnet is a clear circular quartz inclusion. There is no evidence of subgrain development or lattice distortions surrounding this quartz grain. (b) A partial electron channeling pattern for a dumb-bell-shaped garnet grain from sample 3164-2. Note the total lack of subgrains or distortion in the diffraction pattern, indicating a lack of any of the indicators of internal strain.

crystallographic preferred orientation) are also observed in the deformed garnet-bearing quartzites. Two examples of optically measured *c*-axes patterns are shown in Fig. 8(a). Compared to typical granulite patterns the girdles seem to be more reduced to individual maxima, probably an effect of the strong static grain coarsening. Crossed-girdle textures of this type have been modeled by Lister (1979, 1981) and generally are interpreted to result from combined activity of basal-<*a*> and prism-<*c*> slip systems. This is compatible with the observed subgrain pattern, although the subgrain pattern is not necessarily related to the high-strain event.

For the quartzes which surround and include the deformed garnets, complete crystallographic data were measured by ECP-pattern analysis (Fig. 8b). Due to the extreme grain size as compared with the relatively small sampling area of the SEM sample only few points ($N = 54$) were measured and multiple measurements of one grain could not be excluded. Therefore, only a few maxima are developed instead of girdles and also the asymmetrical distribution of maxima in the pole figures is thought to be an artificial effect. A high degree of position-switching between *c*- and *a*-axis maxima orientations in the XZ plane, indicating that crystals are nearly equally well oriented for either prism-<*c*> or basal-<*a*> slip, assuming a roughly coaxial strain path, is in accordance with the interpretation of the optical measured data. The *c*-axis maximum near the center of the pole figure represents grains favorably oriented to activate prism-<*a*> slip under the same strain path regime.

5.3. Feldspar

Feldspar textures have not been measured, but the preferred orientation of albite twin lamellae close to the foliation indicates that they have a significant CPO with (010) close to the XY plane. This could be explained by the activity of the common [001](010) slip system of plagioclase.

Flame perthites developed from alkali-feldspars usually are oriented at high angle to the foliation and

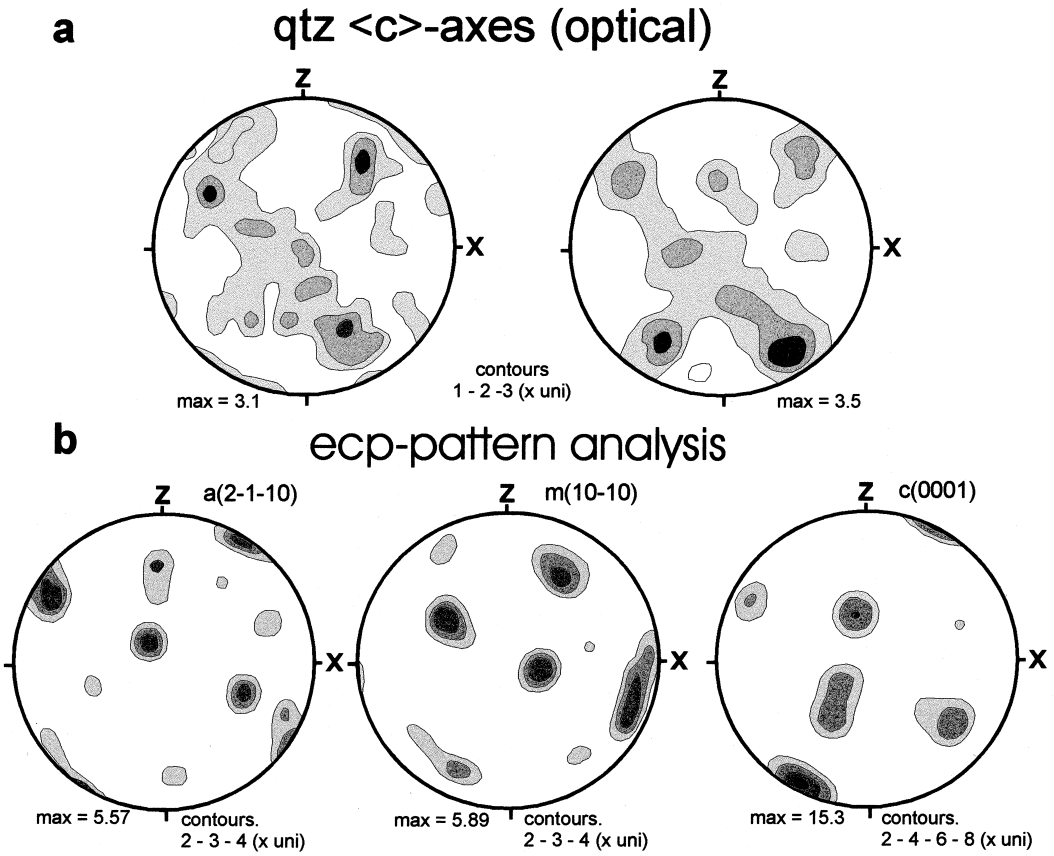

Fig. 8. (a) Quartz *c*-axes preferred orientation measured by universal stage. Both are from sample 3164, the left pattern is from a layer (sample 3164-2) with a quartz grain size of about 2–5 mm diameter in which the garnet texture (Fig. 9) was measured, the right pattern is from a coarse-grained pure quartzite, where grain growth is not hampered by a second phase and grain sizes are on the centimeter scale. Number of measurements is 150 for each diagram. (b) Preferred orientations of quartzes including the deformed garnets measured in Fig. 9 derived from ECP-pattern analysis. Number of measurements is 54, but due to the large grain size multiple measurements of single grains are probable.

stretching lineation. Pryer et al. (1995) showed that these are crystallographically oriented (growing in the plane of minimum misfit between K-feldspar and albite), and therefore one can conclude that the alkali-feldspars also show a distinct CPO.

5.4. Garnets

If the shape of the garnets is due to intracrystalline strain by dislocation glide, a crystallographic preferred orientation should result. Because garnets are optically isotropic due to their cubic symmetry, their crystallographic preferred orientation cannot be measured by U-stage methods, strengthening the reliance on SEM based methods. ECP analysis was performed on sample 3164, which showed numerous deformed garnets strongly aligned parallel to the stretching lineation. Garnets from this sample are extremely homogeneous compositionally, with an average composition of Alm 84% Prp 13.7% Sps 2.0% based on electron probe analysis. These grains were indexed using an ECP map for end-member almandine with the assistance of the indexing program Channel (Schmidt and Olesen, 1989).

In contrast with previous reports (Kleinschrodt and McGrew, 1995; Kleinschrodt, 1996b) a new analysis of an extended data set reveals a distinct crystallographic preferred orientation of the garnets (Fig. 9a). The $<111>$ axes distribution shows a significant maximum in the stretching direction and the other maxima are arranged in girdles at an angle of 70° to X. The (110) poles show numerous maxima, including one normal to the foliation. The others are arranged on a central girdle normal to X and two small circle girdles at an angle of about 30° to X. The (100) poles form distinct maxima that lie on girdles at about 45° to X. Comparing these results with the orientation of the respective axes of a garnet single crystal with one (111) direction in the stretching lineation and one (110) plane in the foliation (Fig. 9b), the distribution of (111), (110) and (100) poles fits the distribution of maxima in the sample remarkably well. These results strongly argue for the $1/2<111>\{\bar{1}10\}$ slip systems being responsible for the preferred orientation of the

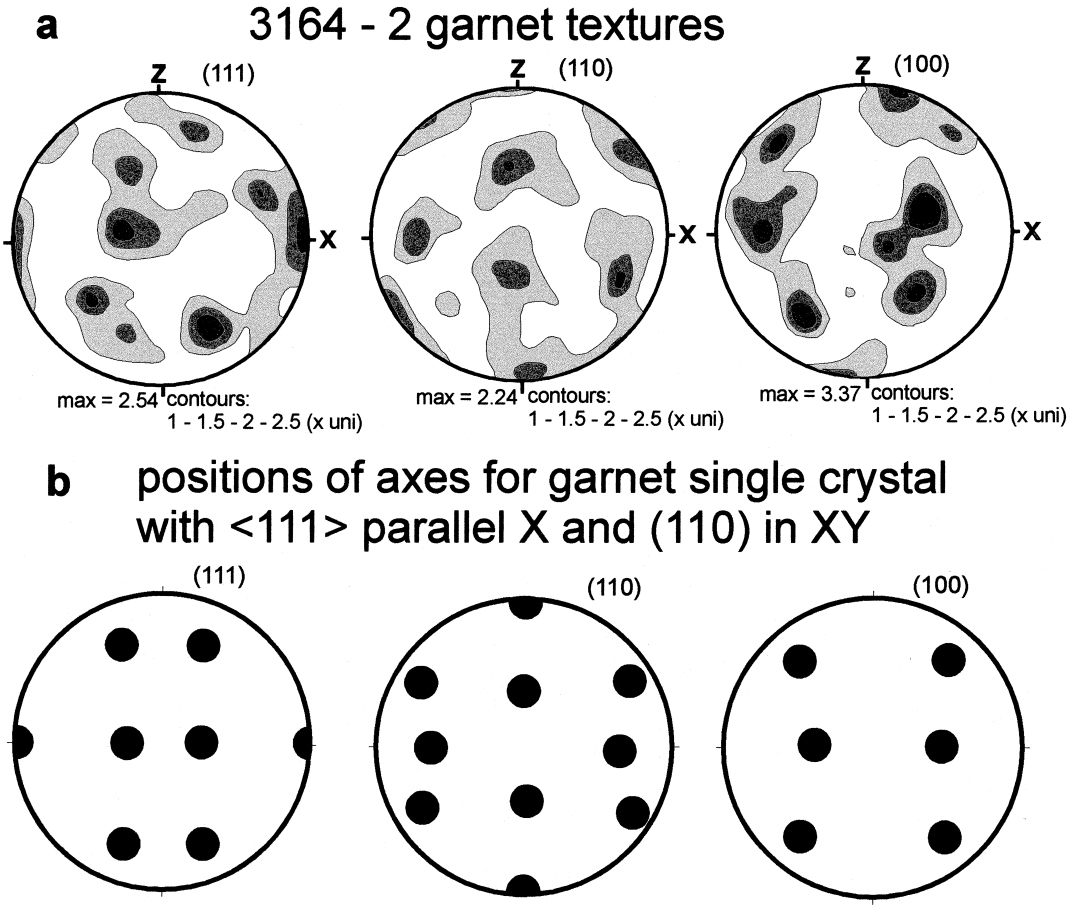

Fig. 9. (a) Garnet textures of sample 3164-2 derived from ECP analysis. Stereographic plots (lower hemisphere) for (111), (110) and (100) displayed in XZ-sections. (b) Positions for (111), (110) and (100) of garnet with $<111>$ oriented parallel to the stretching lineation and a (110) plane in the foliation (including symmetrically equivalent positions).

garnets, which is regarded as the slip system that is easiest to activate (Voegele et al., 1998).

In contrast with the reports on intracrystalline deformation structures (subgrains) arguing for dislocation creep (Prior et al., 1996, 1998) few or in most cases no subgrains can be found within the garnets as revealed by orientation contrast imaging (Fig. 7). Fig. 7 shows the grain with the most extensive subgrain development, but even in this case, subgrains are large. ECP bands within such subgrains are sharp, straight and distinct. Note that this grain also contains a round quartz inclusion, but shows absolutely no evidence for distortion of the crystal lattice in the vicinity of the inclusion or the existence of subgrains related to strain in the vicinity of the inclusion. Similar round quartz inclusions were also described by Ji and Martignole (1994). Their explanation is that quartz is much stronger than garnet and behaves as a rigid inclusion in the garnet. However, because the microstructural observations reported above show that garnet is still the strongest phase, this explanation cannot be correct. The round quartz grains are usually found in larger garnets with moderate strain. In particular, we have never found quartz in regions of necking. On the contrary, some observations indicate that if quartz is included in such positions then the garnet cracks at this site. Therefore, the quartz inclusions probably were only slightly strained and may have rounded their shapes slightly during the static high-T annealing.

Even 'dumb-bell'-shaped grains show identical crystallographic orientations between the two halves of the grains, with no evidence of any lattice distortion or subgrain development in the 'neck' regions where one would expect strain to be most intense. Locally, nearby grains (like those shown in Fig. 4d) show nearly identical crystallographic orientations, suggesting that they were boudinaged and detached from an original parent grain without experiencing substantial relative rotation. Thus, there remain the conflicting observations of deformational microstructures and preferred crystallographic orientation, but few signs of plastic internal deformation.

6. Discussion and interpretation

The garnets from Sri Lanka seem to be unique as compared to other reports to date, because they preserve deformation features such as pinch and swell structures and microboudinage in addition to high aspect ratios. The garnets described by Ji and Martignole (1994) are lensoid and just one of their examples shows a slight pinch and swell structure. Older reports on elongate garnets show either highly 'flattened' garnets whose shapes are clearly reaction controlled (Blackburn and Dennen, 1968), or garnets that are only slightly elongated and therefore may be growth controlled (Dalziel and Bailey, 1968). In contrast, we believe that the deformation features shown in Fig. 4 can only be explained by plastic deformation of the garnets. The necking structures argue for a slightly higher flow strength of garnet compared to the quartz matrix.

An important question is whether the garnets really were round objects prior to plastic deformation or whether they had an initial non-spherical shape, that is, are the aspect ratios a measure of strain during plastic deformation or did the garnets have an initial shape anisotropy which was overprinted by later plastic strain? There are some indications that small elongate garnets may result from larger garnets by fragmentation and drifting apart of the fragments in the ductile quartz matrix. So in some examples fragments still stick together and show significant elongate shapes. This could be a mechanism to reduce the grain size of garnets and cause a tabular shape prior to plastic deformation.

The strain derived from the aspect ratios on the other hand seems to be in a reasonable relation to the strain determined from deformed feldspar and magnetite grains (Figs. 2 and 3). However, these probably also were not isotropic in shape prior to deformation. As no one would doubt plastic deformation of the feldspars (Fig. 3c) and magnetite (Fig. 4a, c) the similar features of garnets in these samples argue for a similar origin.

Most publications on garnet plasticity argue for deformation by dislocation slip or recovery accommodated dislocation slip being the dominant deformation mechanism during natural garnet deformation in the crust and upper mantle (Ji and Martignole, 1994; Karato et al., 1995). Recent work demonstrated that garnets commonly show numerous subgrains even where no significant strain can be derived from their shape. Usually such garnets show no CPO (Prior, personal communication).

The significant data provided by our example are:

1. There are few microscopic or submicroscopic deformational features in the garnets to argue for dislocation creep being a dominant factor. The garnets of Ji and Martignole (1994) show numerous dislocations, dislocation arrays and networks in subgrain boundaries, which is their main argument for recovery-accommodated dislocation creep. They argue for very high-temperature deformation of the garnets in the contact aureole of the Morin Anorthosite massif at temperatures above 900°C. Later, the rocks have been overprinted in the Morin shear zone at temperatures of 550–750°C. The later deformation is preserved in the quartz microfabric

surrounding the garnets with subgrains, undulatory extinction and dynamic recrystallization. According to the interpretation of Ji and Martignole (1994, 1996) the garnets exclusively reflect the high-temperature deformation. As the Sri Lankan garnets, which were deformed at temperatures between 750 and 850°C, show none of these features, it seems likely that the dislocation substructures in garnets of Ji and Martignole may not have been related to the deformation causing the significant aspect ratios, but rather may have been created during activity of the Morin shear zone in connection with only minor intracrystalline strain. Ji and Martignole exclude this possibility because 'temperatures from 550–750°C... are too low to cause garnet to be softer than quartz and feldspar'. The statement that garnet is softer than quartz and feldspar is derived from the more oblate shape of the strain ellipsoid of garnet according to Freeman and Lisle (1987), which seems not to be a reliable argument (see discussion above). And if garnet is not softer than quartz, but slightly stronger it probably can acquire a limited number of dislocations under these lower T conditions, though not enough to drive recrystallization.

2. According to the aspect ratio/grain-size correlation, deformation must be related to a grain-size sensitive deformation mechanism, with weakening correlating to lower grain size. The reduction in grain size of larger garnets is achieved by fracturing and shear sliding. Even though larger garnets usually also show a slight shape preferred orientation in the quartzites, significant elongation and the well-developed features of deformation shown in Fig. 4 are restricted to small grain size (less than 0.4 mm^2).
3. The garnets show a distinct crystallographic preferred orientation and the pattern indicates the dominance of the $1/2 <111> \{110\}$ slip system. This is the first report of clear CPO patterns in garnet. There have been several reports on preferred orientations in garnet (Weber, 1997; Mons and Paulitsch, 1969), but the CPOs were weak and difficult to interpret. A common argument for this is that in cubic minerals due to the high number of independent slip systems no distinct preferred orientation pattern will develop (e.g. Ji and Martignole, 1996). Our example shows that under appropriate conditions garnets develop a distinct pattern with the slip direction aligned with the stretching lineation (X) and the slip plane in the foliation plane (XY). Yet, the scarce intracrystalline deformation features in the garnets seem to contradict such an interpretation. An explanation for this feature could be that annealing and very slow cooling from high temperatures causes a complete healing of all such intracrystalline defect structures. The same obviously happens to quartz, which frequently forms grains with completely homogeneous extinction in thin sections. These quartz grains also have distinct CPOs with typical high-temperature, 90° crossed girdles arguing for dislocation creep with combined basal-$<a>$ and prismatic slip systems. Coarse subgrains present in quartz may be acquired by low stresses during cooling.

The grain-size sensitivity is also not to be expected for a dislocation creep mechanism. Yet, due to the very large Burgers vector, dislocation creep in garnet may differ from the same process for example in quartz. In their experimental approach to garnet plasticity, Voegele et al. (1998) propose a mechanism of diffusion-assisted dislocation glide as a possible mechanism to overcome the problem of the high Peierls force of the dislocations in the garnet structure. According to their model, local diffusion of point defects is necessary to displace the sessile component of the large dislocation core. Our observations also point towards a combination of dislocation creep with diffusion mechanisms, which may provide an explanation for the observed grain-size sensitivity.

Den Brok and Kruhl (1996) suggested Coble creep/pressure solution as a possible mechanism. However, a pressure solution type mechanism is unlikely, as the rocks seem to be essentially dry and show no sign of partial melting under these conditions. IR-spectroscopy shows nearly no free detectable water in these dry granulite facies quartzites. Furthermore such a mechanism cannot explain the preferred orientations described in this paper. Therefore a diffusion-assisted dislocation creep model is much more realistic than a solution/precipitation process.

6.1. Flow strength between garnet, quartz and feldspar

Ji and Martignole (1996) agree that currently available experimental data on plastic deformation of dry quartz, feldspar and garnet are not sufficient to reliably recalculate the flow strength of these minerals at high temperature. Yet, their attempt on the basis of the existing data at least shows that the differences in flow strength become very small at high temperature. Based on recent experiments on natural garnets and the flow-law parameters of Gleason and Tullis (1995) for quartz and Shelton and Tullis (1981) for feldspar, Wang and Ji (1999) concluded that garnet is slightly stronger than quartz and feldspar, and feldspar stronger than quartz at temperatures of 800–900°C. Our observations affirm the small viscosity contrast between garnet, dry quartz and feldspar. However, comparison of finite strain among these three phases leads us to conclude that garnet is the strongest phase, quartz is a little weaker, and feldspar is the weakest. The main

argument for this is that garnet is deformed in a quartz matrix, but nearly undeformed in a feldspar matrix. This discrepancy may be due to the very restricted availability of flow-law parameters for feldspars.

The inversion in flow strength between quartz and feldspar seems not to be significant enough to fundamentally influence whole rock viscosity. Nearly pure quartz layers and feldspar-rich layers are deformed together without any sign of viscosity contrast (e.g. cusps, boudinage) even at very high strains.

6.2. Temperature conditions

Voegele et al. (1998) experimentally determined that temperatures $>1000^{\circ}C$ are required for the onset of garnet ductility. Ji and Martignole (1994) regarded natural garnet deformation as an indicator of 'extremely high temperature deformation', thus being restricted to specific geological situations such as the contact of the Morin Anorthosite.

Since OC images have become available, subgrains were found in garnets down to greenschist facies conditions and prove that dislocations can move in the garnet structure (Prior et al., 1996). Yet such greenschist and amphibolite facies garnets usually show no sign of significant strain. Only at higher temperatures can dislocation creep become effective and produce higher strain, probably as diffusion gets more rapid at such temperatures. The temperatures reached in the Sri Lankan granulites in the structural level where the garnets occur did not exceed 850°C in the range of the reliability of the geothermometric methods (i.e. about $\pm 50^{\circ}C$) (Schumacher et al., 1990; Kleinschrodt and Voll, 1994). Deformation of the garnets follows the thermal peak and can be constrained to a temperature of 750–850°C. It is to be expected that ductile deformation of garnet occurs more frequently in granulites deformed at temperatures above 800–850°C. As we have pointed out, the subtle differences in flow strength between quartz, feldspar and garnet at high temperatures in our example is just enough to allow significant deformation of garnet in a quartz matrix and in all the examples we have found so far such deformational features in garnet have been found exclusively in a quartz matrix.

7. Summary

Based on the above observations and data set, we summarize the main conclusions:

1. Garnet can be plastically deformed under quite normal granulite facies temperatures (750–850°C)
2. Garnet is deformed by a diffusion-assisted dislocation creep mechanism.
3. Reduction of grain size by fracturing of larger garnets, competes with plastic deformation, and is a prerequisite for diffusion-assisted dislocation creep to become effective.
4. Garnet flow strength > dry quartz flow strength > feldspar flow strength.
5. Significant amounts of strain were only found where garnet is included in a quartz matrix.

Dislocation creep in garnet is difficult under crustal conditions according to experimental data (Karato et al., 1995; Voegele et al., 1998). It has been demonstrated that garnets from different metamorphic rocks (amphibolite facies, eclogites) show numerous subgrains and therefore are deformed by dislocation creep. Yet, usually these substructures are not associated with significant strain in the garnets and show no preferred orientation of the garnets. Our example shows that under common granulite facies temperatures ($800 \pm 50^{\circ}C$) garnets with higher strain and significant CPOs can be found. The observed CPOs indicate the importance of the $1/2 <111> \{110\}$ slip system in garnets deformed under granulite facies conditions.

Acknowledgements

R.K. thanks the German Science Foundation for support during initial states of the work (Project Kl851/1), P.W. Vitanage and his family for their hospitality in Sri Lanka, G. Voll for his initial support to work in Sri Lanka. A.M. wishes to acknowledge funding from National Science Foundation post-doctoral fellowship EAR-9208855. We are especially grateful to Geoff Lloyd, who provided important insights and made available the facilities of the Leeds University electron microscopy laboratory. D. Mainprice helped in the preparation of some pole figures. The critical and constructive reviews by D. Mainprice and D. Prior improved the paper significantly.

References

Blackburn, W.H., Dennen, W.H., 1968. Flattened garnets in strongly foliated gneisses from the Grenville Series of the Gananoque area, Ontario. American Mineralogist 53, 1386–1393.

Dalziel, I.W., Bailey, S.W., 1968. Deformed garnets in a mylonitic rock from the Grenville front and their tectonic significance. American Journal of Science 266, 542–562.

den Brok, B., Kruhl, J., 1996. Ductility of garnet as an indicator of extremely high temperature deformation: Discussion. Journal of Structural Geology 18, 1369–1373.

Freeman, B., Lisle, R.J., 1987. The relationship between tectonic strain and the three-dimensional shape fabric of pebbles in deformed conglomerates. Journal of the Geological Society of London 144, 635–639.

Gleason, G.C., Tullis, J., 1995. A flow law for dislocation creep of quartz aggregates determined with the molten salt cell. Tectonophysics 247, 1–23.

Gregg, W., 1978. The production of tabular grain shapes in metamorphic rocks. Tectonophysics 49, T19–T24.

Hölzl, S., Hofmann, A.W., Todt, W., Köhler, H., 1994. U–Pb geochronology of the Sri Lankan basement. Precambrian Research 66, 123–149.

Ji, S., Martignole, J., 1994. Ductility of garnet as an indicator of extremely high temperature deformation. Journal of Structural Geology 16, 985–996.

Ji, S., Martignole, J., 1996. Ductility of garnet as an indicator of extremely high temperature deformation: Reply. Journal of Structural Geology 18, 1375–1379.

Karato, S., Wang, Z., Liu, B., Fujino, K., 1995. Plastic deformation of garnets: systematics and implications for the rheology of the mantle transition zone. Earth and Planetary Science Letters 130, 13–30.

Kleinschrodt, R., 1994. Large scale thrusting in the lower crustal basement of Sri Lanka. Precambrian Research 66, 39–57.

Kleinschrodt, R., 1996a. Strain localization and large scale block rotation in the lower continental crust, Kataragama area. Sri Lanka. Terra Nova 8, 236–244.

Kleinschrodt, R., 1996b. Plastical deformation of garnet under crustal conditions. European Journal of Mineralogy 8, 143.

Kleinschrodt, R., McGrew, A.J., 1995. Garnet plasticity in the lower continental crust: Constraints on deformation mechanisms from microstructural and textural data. Joural of the Czech Geological Society, C 40 (3), 104.

Kleinschrodt, R., Voll, G., 1994. Deformation and metamorphic evolution of a large-scale fold in the lower crust: the Dumbara synform, Sri Lanka. Journal of Structural Geology 16, 1495–1507.

Kleinschrodt, R., Voll, G., Kehelpannala, W., 1991. A layered basic intrusion, deformed and metamorphosed in granulite facies of the Sri Lanka basement. Geologische Rundschau 80, 779–800.

Kröner, A., Cooray, P.G., Vitanage, P.W., 1991. Lithotectonic subdivision of the Precambrian basement of Sri Lanka. In: Kröner, A. (Ed.), The Crystalline Crust of Sri Lanka, Part I. Geological Survey Department Professional Paper, 5, pp. 5–21.

Lister, G.S., 1981. The effect of the basal-prism mechanism switch on fabric development during plastic deformation of quartzite. Journal of Structural Geology 3, 67–76.

Lister, G.S., 1979. Fabric transitions in plastically deformed quartzites: competition between basal, prism and rhomb systems. Bulletine de Mineralogie 102, 232–241.

Lloyd, G.E., 1987. Atomic number and crystallographic contrast images with the SEM: A review of backscattered techniques. Mineralogical Magazine 51, 3–19.

Lloyd, G.E. 1994. An appreciation of the SEM electron channeling technique for petrofabric and microstructural analysis of geological material. In: Bunge, H.J., Siegesmund, S., Skrotzki, W., Weber, K. (Eds.), Textures of Geological Materials. DGM-Informationsgesellschaft, Germany, pp. 109–126.

Mons, W., Paulitsch, P. 1969. Garnet orientations in different metamorphic facies. In: Paulitsch, P. (Ed.), Experimental and natural rock deformation. Springer, pp. 100–108.

Prior, D.J., Trimby, P.W., Weber, U.D., Dingely, D.J., 1996. Orientation contrast imaging of microstructures in rocks using forescatter detectors in the scanning electron microscope. Mineralogical Magazine 60, 859–869.

Prior, D.J., Boyle, A.P., Brenker, F.E., Harte, B., Speiss, R., Weber, U., Wheeler, J., 1998. The hidden life of garnet. EOS Transactions, American Geophysical Union spring meeting supplement 79 (17), S356.

Pryer, L.L., Lloyd, G.E., Robin, P.Y.F., 1995. An SEM electron-channeling study of flame perthite from the Killarney Granite, Southwestern Grenville Front, Ontario. The Canadian Mineralogist 33, 333–347.

Ross, J.V., 1973. Mylonitic rocks and flattened garnets in the southern Okanagan of British Columbia. Canadian Journal of Earth Science 10, 1–17.

Schmidt, N.-H., Olesen, N., 1989. Computer-aided determination of crystal-lattice orientation from electron-channeling patterns in the SEM. Canadian. Mineralogist 27, 15–22.

Schumacher, R., Schenk, V., Raase, P., Vitanage, P.W. 1990. Granulite facies metamorphism of metabasic and intermediate rocks in the Highland Series of Sri Lanka. In: Ashworth, J.R., Brown, M. (Eds.), High-Grade Metamorphism and Crustal Anatexis. Allen and Unwin, pp. 235–271.

Schumacher, R., Faulhaber, S., 1994. Summary and discussion of *P–T* estimates from garnet–pyroxene–plagioclase–quartz-bearing granulite-facies rocks from Sri Lanka. Precambrian Research 66, 295–308.

Shelton, G.L., Tullis, J., 1981. Experimental flow laws of crustal rocks. EOS. Transactions of the American Geophysical Union 62, 396.

Voegele, V., Ando, J.I., Cordier, P., Liebermann, R.C., 1998. Plastic deformation of silicate garnet I. High-pressure experiments. Physics of the Earth and Planetary Interiors 108, 305–318.

Voll, G., Evangelakakis, C., Kroll, H., 1994. Revised two-feldspar geothermometry applied to Sri Lankan feldspars. Precambrian Research 66, 351–378.

Wang, Z., Ji, S., 1999. Deformation of silicate garnets: Brittle ductile transition and its geological implications. The Canadian Mineralogist 37, 525–541.

Weber, U.D., 1997. Mikrostrukturen und Texturen in natürlich deformiertem Eklogit: Entwicklung und Anwendung neuer Techniken mit dem Rasterelektronenmikroskop. Diploma Thesis, University of Giessen.